Unsupervised Clustering Uncovers Two Distinct Types of Fixational Eye-Movements in Dynamic Environments

N. W. Heinrich¹, A. Jahanian Najafabadi² and J. Perez-Osorio³

- 1. Dept. of Computer Science & Engineering, Universität zu Lübeck, Lübeck, Germany 2. Dept. Cognitive Neuroscience, Bielefeld University, Bielefeld, Germany
- 3. Cognitive Psychology & Ergonomics, Technische Universität Berlin, Berlin, Germany nils.heinrich@uni-luebeck.de, amir.jahanian@uni-bielefeld.de, j.perez-osorio@tu-berlin.de

Abstract— The present study extends previous work investigating eve-movement control in a dynamic, timeconstrained task environment. Earlier studies showed that the predictability of environmental dynamics influenced fixation allocation and the initiation sites of smooth pursuits. In those experiments, however, eye movements were clustered solely based on whether a reference point fell within foveal or peripheral vision, which may have confounded the analyses. This study introduces a bottomup, data-driven clustering approach to identify fixation types across multiple spatial and temporal dimensions. Six participants steered a spaceship to avoid obstacles under varying levels of motor control uncertainty. We identified two fixation types: Type 0 fixations, which were longer and centrally located near the spaceship, and Type 1 fixations, which occurred farther from the agent and were directed toward more open areas of the screen. Linear mixed modeling revealed that with increasing input noise, Type 0 fixations became shorter and more focused, while Type 1 fixations became longer and shifted farther from nearby obstacles. These patterns suggest adaptive gaze strategies, with Type 1 fixations potentially supporting predictive tracking under high control uncertainty. Our findings provide further evidence of how eye movements flexibly support action in complex, real-time environments.

Keywords—Action control, Eye movements, Adaptive gaze strategy, Unsupervised clustering, Linear mixed modeling

I. Introduction

Action control refers to the cognitive and motor processes that allow humans to select, initiate, and adapt actions in response to goals and changing environments. It involves planning movements, predicting their sensory consequences, and making adjustments based on feedback [1]. In dynamic environments, this process is not linear or pre-scripted: actions are monitored in real time, and behavior is constantly shaped by how well-intended outcomes match actual results. Rather than following a rigid plan, humans adapt their actions on the fly, correct for errors, or abandon goals when needed.

A central component of action control is the visual system. Vision provides real-time information about the environment, allowing humans to plan and guide their actions with precision. During movement, the eyes actively support behavior by anticipating upcoming demands, selecting relevant targets, and monitoring progress [2]. Where we look often reflects our current

goals and, in many cases, even predicts our next actions. This close coupling between gaze and motor control has been demonstrated across a wide range of tasks, from simple everyday activities like tea-making [3] to complex behaviors such as driving [4, 5] (for a review, see Hayhoe & Ballard, 2005 [6]). In such contexts, gaze not only signals intention but also enables rapid corrections and flexible adjustments, particularly when the environment changes unexpectedly. Moreover, beyond guiding our own actions, gaze plays a crucial role in predicting the actions of others [7].

Eye movements serve multiple roles during action control. At times, fixations support immediate motor guidance, for example, by locking onto a target that the hand or body is moving toward [8]. In other moments, they serve more exploratory functions, scanning ahead to anticipate what is coming next (e.g., an obstacle or a slippery surface) or checking task-relevant features in the periphery (e.g., road markings on a bike lane). Rather than sticking to a single function, gaze constantly switches between these roles depending on the demands of the task. In stable and predictable environments, visual guidance often dominates, with the gaze closely tracking the current goal. But as tasks become more challenging or when uncertainty increases, exploratory sampling becomes more prominent. In such cases, eye movements reflect not just ongoing actions but also internal processes like planning, monitoring, or even doubt. The balance between these roles potentially offers insights into how humans implement action control strategies to proactively respond to moment-to-moment changes of their environment.

In the present study, we use a continuous, dynamic task with systematically varied levels of predictability to investigate how gaze supports flexible action control in a complex yet controlled setting. Participants steer a spaceship through an environment featuring obstacles and unpredictable steering, input noise, requiring continuous adjustments in their action control. Eye movements were recorded at high sampling rates, tracking rapid shifts in gaze allocation. With this setup, we explored how gaze shifts between guiding immediate actions, anticipating upcoming demands, and adapting to uncertainty in real-time.

This work extends on previous studies using the same task environment. In Abalakin et al. (2024) [9], we manipulated the predictability of environmental drift, a passive displacement of the spaceship that was either visually indicated or not. We found that fixational eyemovements converged toward an optimal distance from the spaceship when the drift was visible (predictable), whereas invisible (unpredictable) drift prevented such adaptation. In Heinrich et al. (2024) [10], unpredictability in steering was varied on a smaller scale with less distinct levels than in the present study. There, we identified smooth pursuit eye-movements that moved through the environment and typically terminated closer to the spaceship than when they were initiated. These pursuits were initiated closer to the spaceship under mild steering uncertainty but farther away under moderate steering uncertainty. In both studies, fixational eye movements were clustered solely based on whether the spaceship fell within the foveal/parafoveal region or the peripheral field.

Building on these findings, the present study extends the manipulation of input noise and introduces a bottomup, data-driven clustering approach to identify fixation types from multiple spatial and temporal dimensions. With this, we are aiming for a more comprehensive characterization of how gaze supports real-time action control under varying levels of motor uncertainty.

II. METHODS

This study was approved by the ethics committee of the Technische Universität Berlin (proposal KMDS-WS-01-20190814-E2). Six students at the University of Potsdam were recruited through SONA system. All participants had either normal or corrected-to-normal vision (with contact lenses) and no known history of neurological disorders. Before the experiment, informed consent for research and publication was obtained from all individuals. To prevent potential biases, participants were not briefed on the study's hypotheses but only about the task itself. Participants were compensated with 1.5 participation hours.

II-A. Experiment and Procedure

We used the same experimental environment as in our previous studies: **Dodge Asteroids**, a custom environment built in Python [11] using the PyGame library [?]. The environment runs at 60 FPS and builds on a simulation framework originally developed by Kahl et al. (2022) [12] to evaluate a computational model of action control. Dodge Asteroids provides a well-controlled yet dynamic setting, where the environment changes independently of the agent's behavior, while still allowing the agent to act freely and select sub-goals. This combination makes it particularly well suited for investigating the temporal dynamics of action control. Paired with high-frequency eye tracking, the environ-

ment allows us to examine how the statistical properties of action goals evolve in response to increasing uncertainty in the agent's world model [9] or loss of motor control [10, 13].

Obstacles are scattered throughout the environment, with their x- and y-positions drawn from a uniform distribution bound by the width and height of the environment.

Participants steered a spaceship that automatically *falls* through the environment but can be pushed in either horizontal direction using the keyboard (Y = left, M = right; QWERTZ layout). The task was to reach the bottom end without crashing into obstacles.

The Dodge Asteroids environment had a width of 720 pixels and a height of 13,500 pixels. Free fall was 6 pixels each frame. Spaceship and obstacles were 36 pixels in width and height. At any moment during gameplay, only a small part of the full environment, the observation space, was visible (see left side of Figure 1 a). A full example layout is shown on the right of Figure 1 a.

We manipulated the accuracy with which the spaceship is steered by means of *input noise*. Each frame, a key is down to steer the spaceship, its' horizontal displacement is drawn from a normal distribution centered above 6 pixels and with varying standard deviation. Increasing standard deviations impose increasing uncertainty in motor control. There were 5 levels of input noise given by the standard deviations of 0 (no noise, i.e., accurate control), 0.5, 1.0, 1.5, and 2.0.

The experiment was presented on a 28" ASUS PB277Q screen with a 1920x1080 resolution and a refresh rate of 60Hz (equal to the FPS of the Dodge Asteroids environment). Participants were seated with their heads stabilized on a chin rest positioned 80cm from the screen. Eye movements were recorded using a ViewPixx TRACKPixx eye-tracker (VPixx Technologies, Saint-Bruno, QC, Canada), which tracked both eyes at a sampling rate of 2,000Hz. The setup was mounted on a height-adjustable table, ensuring the chin rest and participants' faces remained at a consistent height relative to the screen. The spaceships' position on the screen was kept constant as a static reference point, fixed at coordinates x = 954 and y = 270 pixels (position of the upper left corner of the sprite). Consequently, any movement in the environment, whether due to free fall or steering, caused the surroundings to move relative to the spaceship at the screen center. New objects appear at the bottom of the screen and travel upwards until exiting at the top, taking approximately 2.45s from bottom to top. A gray bar, 270 pixels in height and spanning the full screen width, was displayed at the bottom to discourage gaze shifts beyond the screen (in

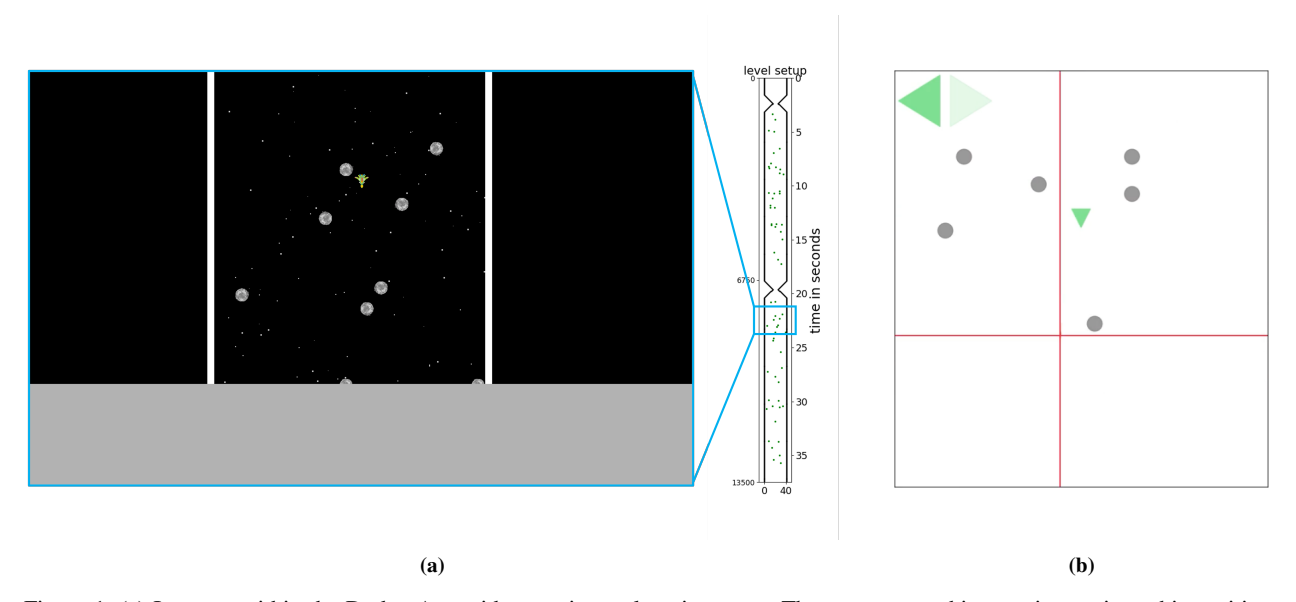


Figure 1. (a) Instance within the Dodge Asteroids experimental environment. The green spaceship remains static at this position on the screen. Obstacles are spread throughout the instance. The full layout of this trial is shown on the right. (b) Simplified representation of a (different) instance within the Dodge Asteroids environment. Here, the participant is steering to the left, indicated by the bright green-colored triangle in the upper left corner. The red cross marks the gaze position.

the flight direction of the spaceship and where new objects appear).

Before the experiment was conducted, we generated 6 distinct environment layouts by randomly placing 62 obstacles (sampling x- and y-positions from a uniform distribution as described above). Participants completed each layout under all five input noise levels, resulting in 30 unique combinations of layout and noise condition.

Prior to every session, the eye-tracker was calibrated individually for each participant using a 9-point grid. Participants then completed a training level measuring 36,000 pixels in length to familiarize themselves with the task. After training, participants solved the 30 unique combinations of layout and input noise that were presented in a randomized order. If a participant crashed during a trial, the same combination was reintroduced later in the session. Each combination could be attempted up to three times. However, combinations that resulted in three consecutive crashes were removed from the participant's remaining sequence. This procedure was designed to prevent the learning of specific obstacle patterns through repetition. Prior to each new trial, a 5point eye-tracker recalibration was performed, allowing participants to take short breaks in between trials during which they could disengage from the chin rest if needed. Both the 9-point and 5-point calibrations were only accepted if the mean error of both eyes during validation was below 50 pixels. Otherwise, the calibration was repeated. Participants completed the experiment in roughly 60 minutes.

For the present analyses, we considered only trials without crashes, since crash trials end prematurely, affecting fixation counts and durations, and fixations just before crashes may involve distinct action-related processes; these will be examined in a separate study.

III. DATA ANALYSIS

Fixation detection was performed as follows. We identified saccades in the dataset using an established velocity-based detection algorithm [14, 15]. A sample was classified as part of a saccade if the eye moved with a velocity of at least 0.5° for four or more consecutive samples ($\geq 0.002s$), with the velocity threshold determined using a multiplier of $\lambda = 6$. Periods in which either eye signal was lost were labeled as blinks. Blinks, as well as the events directly preceding or following a blink (i.e. fixations or saccades), were excluded from further analysis. Finally, fixations were defined as time intervals between consecutive saccades. In total, we identified 31,505 fixations on the basis of which we conducted the analyses described below.

Briefly going over the structure of the data, each row is a fixation which is linked to its distance to the spaceship in visual degrees, its fixation duration in seconds, its distance to the closest obstacle in visual degrees, and the input noise in the trial the fixation occurred.

All data processing and analyses were conducted using Python (v3.9.18), and relevant scientific libraries

(numpy [16] and pandas [17]). For reproducibility of our results, we used a random seed(36)¹.

III-A. Principal Component Analysis

Principal Component Analysis (PCA) was applied using the scikit-learn (sklearn) library [18] to explore the structure of visual and spatial information related to participants' fixations during spaceship navigation. PCA is an unsupervised dimensionality reduction method that identifies orthogonal components maximizing the variance in the feature space, without reference to any target variable. We entered three features: distance to the spaceship, fixation duration, and distance to the closest obstacle. All features were z-standardized prior to the analysis.

The PCA yielded three orthogonal components that together explained 100% of the total variance in the projected data, with individual components accounting for 39.9%, 33.2%, and 26.9%, respectively. Since each component explained a substantial portion of the variance, all three components were kept for the clustering analysis described in the next section.

III-B. Quantile-Based Clustering

We applied quantile-based clustering [19] to the three identified features using the QuClu library. Here, data points were assigned to the closest quantile (or a weighted sum of quantiles in higher dimensions). We chose this clustering method over standard clustering techniques (e.g., k-means) because it is more robust to outliers and non-Gaussian or skewed distributions and allows for variable-wise scaling and quantile normalization [20]. This makes quantile-based clustering especially beneficial for fixation data, where feature distributions often exhibit heavy tails, unequal scaling, and non-linear effects.

Clustering was performed with B=50 resamplings to ensure stability of the quantile estimates. The number of clusters K was varied from 2 to 10. For each k, we computed the silhouette score, a standard internal validity index that quantifies how well-separated and cohesive the resulting clusters are (Figure 2). The highest silhouette score was obtained for K=2, suggesting that the fixation data consists of two types of fixations.

All fixation events were assigned to the distinct fixation types based on the resulting clusters (Type 0 and Type 1). Next, two fixation types were described based on their original feature values, highlighting the differences in spatial and temporal fixation patterns. Following the descriptive analysis, we investigated whether these types

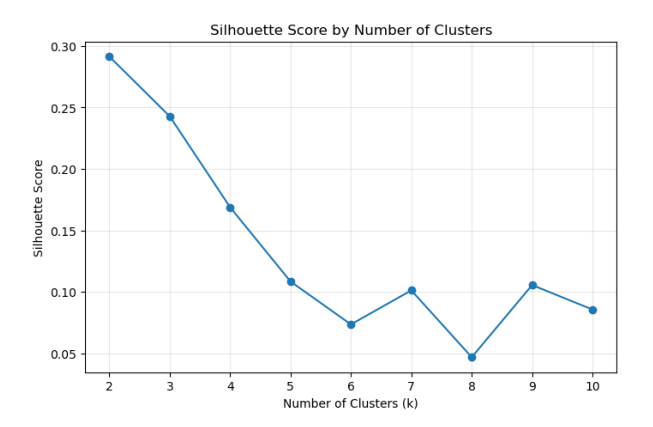


Figure 2. Silhouette scores (y-axis) for fixation data clustered into various number of clusters (x-axis).

also show distinct sensitivity to input noise using linear mixed modeling.

III-C. Descriptives

There could be a general difference in how often fixations of the different types are initiated. Therefore, we calculated the total number of fixations per fixation type for each trial, resulting in one data point per trial and fixation type ($N_{\rm fix,0}$ and $N_{\rm fix,1}$). The mode of Type 0 fixations per trial, estimated using kernel density estimation (KDE), was 22.525. For Type 1 fixations, the mode was 29.253 fixations per trial.

Type 0 fixations featured a mean distance to the spaceship of 2.544° (1.489), a mean fixation duration of 0.240s (0.370), and a mean distance to the closest obstacle of 3.305° (1.920).

Compared to Type 0 fixations, Type 1 fixations featured a greater mean distance to the spaceship of 8.198° (2.473), a shorter mean fixation duration of 0.178s (0.363), and a greater mean distance to the closest obstacle of 4.241° (1.917).

Note that the distributions of all variables of interest are skewed to the right, with more probability density gathered in the right tail compared to the left tail (Figure 3). To mitigate potential violations of model assumptions, we explored appropriate data transformations before proceeding with linear mixed modeling.

III-D. Linear Mixed Modeling

Box-Cox distributional analyses were conducted [21] using the scipy.stats library [22] for data transformation. Applied transformations and corresponding lambda values are stated in the individual paragraphs. Linear mixed models were built using the statsmodels.formula.api library [23] and in every model, the participant ID was entered as a random

¹Git repository containing experimental data and Jupyter Notebook (Clustering&Analysis.ipynb) with code for all analyses described in this paper.

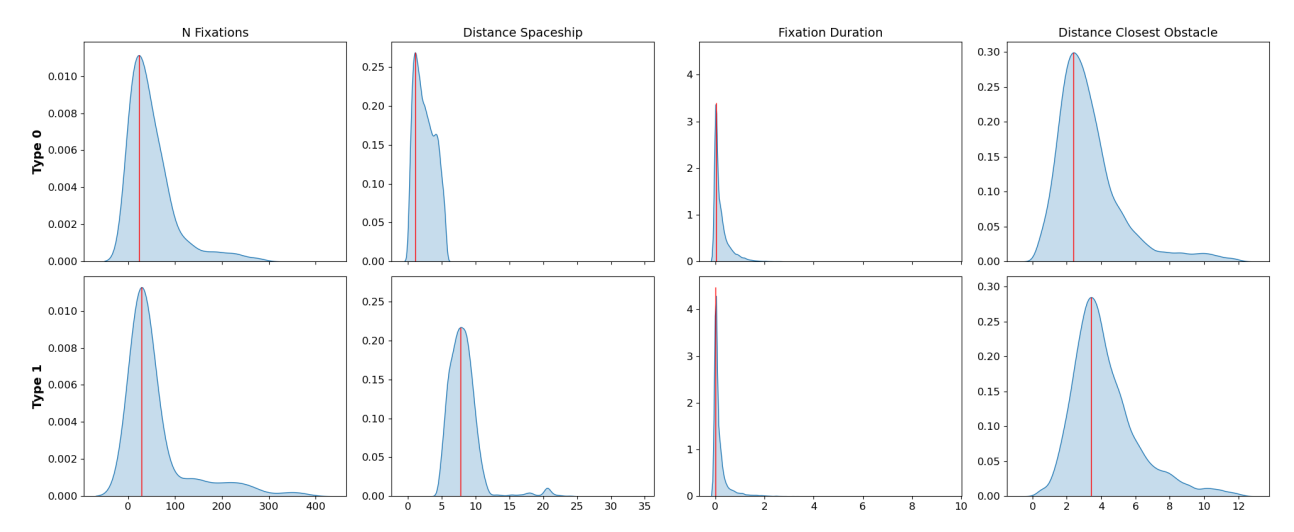


Figure 3. Kernel density estimates (KDEs) for 4 different metrics (columns) of Type 0 and Type 1 fixations (rows) identified through quantile-based clustering. The first column shows the number of fixations of the respective type in a given trial. Columns 2 to 4 are the metrics based on which the 2 fixation types were identified in the clustering process.

intercept effect and input noise as a numerical fixed effect.

First, we investigated whether the number of fixations of each type varies systematically with input noise, under the hypothesis that different fixation types i.e. their roles become more or less relevant as uncertainty in motor control increases. $N_{\rm fix,0}$ was log transformed (λ = 0.239). The number of Type 0 fixations decreased with increasing input noise (β = -0.181, σ = 0.079, 95% CI - 0.335 - -0.027, p = .021). $N_{\rm fix,1}$ was also log transformed (λ = 0.042). We also found a significant decrease in the number of fixations with increasing input noise (β = -0.415, σ = 0.069, 95% CI -0.550 - -0.279, p < .001).

We then turned to more detailed analyses, using individual fixations as data points for the respective cluster. Each fixation was linked to its specific characteristics (distances to objects on the screen and its' duration) and the input noise level of the trial during which it occurred.

Type 0 fixations' distance to spaceship in visual degrees was square root transformed ($\lambda = 0.539$). We found that the higher the input noise level was, the closer Type 0 fixations were allocated to the spaceship ($\beta = -0.023$, $\sigma = 0.006$, 95% CI -0.035 - -0.012, p < .001).

A reciprocal transformation was applied to the distance to the spaceship in Type 1 fixations (λ = -0.909). There was no significant effect of input noise on distance to spaceship (β = -0.001, σ = 0.000, 95% CI -0.001 - 0.000, p = .248).

Fixation duration of Type 0 fixations was log-transformed ($\lambda = 0.093$). Input noise had a significant

negative effect (β = -0.097, σ = 0.018, 95% CI - 0.132 - -0.063, p < .001), meaning that the higher the uncertainty in motor control was, the shorter Type 0 fixations lasted.

Type 1 fixations' duration was also log-transformed (λ = -0.017). Contrary to the effect of input noise in Type 0 fixation duration, increasing input noise was associated with longer fixation durations (β = 0.043, σ = 0.016, 95% CI 0.011 - 0.075, p < .009).

We log-transformed the distance to the closest obstacle of Type 0 fixations ($\lambda = 0.163$). Input noise had no significant effect on the variable of interest ($\beta = -0.001$, $\sigma = 0.007$, 95% CI -0.014 - 0.013, p = .981).

For the distance to the closest obstacle in Type 1 fixations, the Box-Cox distributional analysis also indicated a log transformation ($\lambda=0.246$). Increasing input noise was associated with longer distances to the closest obstacle ($\beta=0.034,\ \sigma=0.005,\ 95\%$ CI 0.023 - 0.044, p < .001).

IV. DISCUSSION

With the experiment described here, we continue a series of experiments investigating the relationship between oculomotor control and action control. Participants navigated a spaceship through a dynamic but well-controlled environment, attempting to avoid collisions with obstacles while dealing with varying levels of motor noise that impaired their control. We recorded their eye movements throughout gameplay to investigate how gaze supports action control under uncertainty. Based on the assumption that fixations serve different functional roles during action control, we expected that distinct types of fixations could be distinguished statistically. We

therefore applied quantile-based clustering and analyzed the obtained clusters using linear mixed modeling.

Type 0 fixations were initiated less often in a trial than Type 1 fixations. In both fixations types, the number of fixations decreased with increasing input noise.

Type 0 fixations were generally closer to the spaceship and longer in duration than Type 1 fixations. As input noise increased, they became even more tightly focused on the ship and decreased in duration. Their distance to the nearest obstacle, however, remained unaffected. These fixations may be used to monitor the regions in the immediate vicinity of the spaceship, and the effects of input noise indicate that monitoring becomes more rigorous with heightened demands on real-time motor control. Interestingly, the spatial pattern of Type 0 fixations resembles the center bias in fixations reported by Burlingham et al. (2024) [24]. In the context of our task, Type 0 fixations are allocated near a central reference point, potentially to optimize energetic efficiency, particularly under conditions of control loss or increased task difficulty.

Type 1 fixations, in contrast to Type 0, tended to occur farther from both the spaceship and the nearest obstacle and were shorter in duration. As input noise increased, these fixations were allocated even farther from obstacles and became longer in duration, while their average distance to the spaceship remained stable. Notably, they were often directed toward relatively empty regions of the screen, as indicated by their greater distance from nearby obstacles. This spatial pattern suggests that Type 1 fixations may serve to track anticipated target locations, the positions of which change over time due to the dynamic visualization of the task. In line with this interpretation, our findings appear to recover the two types of fixation roles described in Lisberger (2015) [8], with Type 0 fixations anchored near the spaceship and relying on peripheral vision to monitor environmental features, while Type 1 fixations are more directly locked onto target positions. Moreover, the increasing distance to obstacles under higher input noise, when control outcomes become more uncertain, may reflect an adaptive, forward-looking gaze strategy aimed at reducing risk by gathering information about future action-relevant locations.

If Type 1 fixations are directed toward target positions, and these target positions move because the environment shifts around a spaceship that remains centered on the screen, then they are not fixations in the strict sense. Rather, they likely represent smooth pursuit eye movements, with their velocity corresponding to the motion of anticipated target positions across the screen (similar to the *foveated action goals* described by Heinrich et al., 2024 [10]). Smooth pursuits can directly support motor behavior, as the pursuit signal itself may be sufficient

to improve (hand) motor control during interactions with moving objects [25]. This characteristic could be another distinguishing feature between Type 1 and Type 0 fixations. Type 0 fixations are primarily directed at the spaceship itself, an object whose position remains stable on the screen, and thus would not elicit smooth pursuit. Investigating whether Type 1 fixations indeed exhibit smooth pursuit-like properties could be a valuable direction for future experiments.

Beyond their role in efficient visuomotor control, Type 0 and Type 1 fixations may reflect distinct modes of self-environment coupling. Stable, Type 0 fixations help maintain a coherent perceptual anchor and predictable sensory input, whereas Type 1, pursuit-like fixations support adaptive engagement with dynamically changing action goals. Smooth pursuits rely on predictive mechanisms, such as corollary discharge, to maintain accurate tracking once the fovea is stabilized on a moving target, and disrupted predictive signals can impair pursuit performance [26]. This functional distinction suggests that the balance between Type 0 and Type 1 fixations may be critical for efficient action control: Type 1 fixations allow participants to track anticipated target locations, especially when motor control is uncertain, while Type 0 fixations preserve stability when cognitive resources cannot be fully allocated to action selection. Notably, these same perceptual and oculomotor processes are often disrupted in clinical populations, such as patients with schizophrenia and borderline personality disorder, who exhibit unstable self-perception, altered smooth pursuit, and difficulties maintaining spatial anchoring. Our classification framework could thus provide a computational or behavioral marker of how efficiently individuals balance sensory stability and goaldirected engagement, a balance that appears perturbed in disorders involving self-disturbances.

This study may present a novel approach to studying eye movements in dynamic, time-constrained environments. It is inspired by scenarios such as natural driving but simplified in terms of complexity and participant behavior (e.g., head movements constrained by a chin rest) for better experimental control. The paradigm combines a screen-based task, where participants freely choose subgoals, with high-frequency eye tracking. With this setup, we explore the functional roles of eye movements in real-time action and how these roles adapt under varying levels of control uncertainty. We are continuously refining the paradigm to validate our findings, and welcome discussions and collaborations.

ACKNOWLEDGMENT

This research was funded by the German Research Foundation (DFG) Priority Program 2134 'The Active Self'. We thank the Potsdam EyeLab team, led by Prof. Ralf Engbert, for their support in data collection.

REFERENCES

- [1] B. Elsner and B. Hommel, "Effect anticipation and action control," *Journal of Experimental Psychology: Human Perception and Performance*, vol. 27, no. 1, pp. 229–246, 2001.
- [2] M. F. Land, "Eye movements and the control of actions in everyday life," *Progress in Retinal and Eye Research*, vol. 25, no. 3, pp. 296–324, 2006.
- [3] M. Land, N. Mennie, and J. Rusted, "The roles of vision and eye movements in the control of activities of daily living," *Perception*, vol. 28, no. 11, pp. 1311–1328, 1999.
- [4] F. I. Kandil, A. Rotter, and M. Lappe, "Driving is smoother and more stable when using the tangent point," *Journal of vision*, vol. 9, no. 1, pp. 11–11, 2009.
- [5] R. M. Wilkie and J. P. Wann, "Driving as night falls: The contribution of retinal flow and visual direction to the control of steering," *Current Biology*, vol. 12, no. 23, pp. 2014–2017, 2002.
- [6] M. Hayhoe and D. Ballard, "Eye movements in natural behavior," Trends in cognitive sciences, vol. 9, no. 4, pp. 188–194, 2005
- [7] J. R. Flanagan and R. S. Johansson, "Action plans used in action observation," *Nature*, vol. 424, no. 6950, pp. 769–771, 2003.
- [8] S. G. Lisberger, "Visual guidance of smooth pursuit eye movements," *Annual review of vision science*, vol. 1, no. 1, pp. 447– 468, 2015.
- [9] N. Abalakin, N. W. Heinrich, A. Österdiekhoff, S. Kopp, and N. Russwinkel, "Allocation of fixational eye movements in response to uncertainty in dynamic environments," *Proceedings* of the Annual Meeting of the Cognitive Science Society, vol. 46, 2024.
- [10] N. W. Heinrich, A. Österdiekhoff, S. Kopp, and N. Russwinkel, "Goal-directed allocation of gaze reflects situated action control in dynamic tasks," *Proceedings of the Annual Meeting of the Cognitive Science Society*, vol. 46, 2024.
- [11] G. Van Rossum and F. L. Drake, "Python 3 Reference Manual," Scotts Valley, CA, 2009.
- [12] S. Kahl, S. Wiese, N. Russwinkel, and S. Kopp, "Towards autonomous artificial agents with an active self: Modeling sense of control in situated action," *Cognitive Systems Research*, vol. 72, pp. 50–62, 2022.
- [13] A. Österdiekhoff, N. W. Heinrich, N. Russwinkel, and S. Kopp, "Sense of control in dynamic multitasking and its impact on voluntary task-switching behavior," *Proceedings of the Annual Meeting of the Cognitive Science Society*, vol. 46, 2024.
- [14] R. Engbert and R. Kliegl, "Microsaccades uncover the orientation of covert attention," *Vision Research*, vol. 43, no. 9, pp. 1035–1045, 2003.
- [15] R. Engbert and K. Mergenthaler, "Microsaccades are triggered by low retinal image slip," *Proceedings of the National Academy* of Sciences, vol. 103, no. 18, pp. 7192–7197, 2006.
- [16] C. R. Harris, K. J. Millman, S. J. van der Walt, R. Gommers, P. Virtanen, D. Cournapeau, E. Wieser, J. Taylor, S. Berg, N. J. Smith, R. Kern, M. Picus, S. Hoyer, M. H. van Kerkwijk, M. Brett, A. Haldane, J. F. del Río, M. Wiebe, P. Peterson, P. Gérard-Marchant, K. Sheppard, T. Reddy, W. Weckesser, H. Abbasi, C. Gohlke, and T. E. Oliphant, "Array programming with NumPy," *Nature*, vol. 585, no. 7825, pp. 357–362, 2020.
- [17] W. McKinney, "Data structures for statistical computing in python," *Proceedings of the 9th Python in Science Conference*, S. van der Walt and J. Millman, Eds., 2010, pp. 56–61.
- [18] F. Pedregosa, G. Varoquaux, A. Gramfort, V. Michel, B. Thirion, O. Grisel, M. Blondel, P. Prettenhofer, R. Weiss, V. Dubourg, J. Vanderplas, A. Passos, D. Cournapeau, M. Brucher, M. Perrot, and E. Duchesnay, "Scikit-learn: Machine learning in Python,"

- Journal of Machine Learning Research, vol. 12, pp. 2825–2830, 2011.
- [19] C. Hennig, C. Viroli, and L. Anderlucci, "Quantile-based clustering," *Electronic Journal of Statistics*, vol. 13, no. 2, pp. 4849–4883, 2019.
- [20] L. A. García-Escudero, A. Gordaliza, C. Matrán, and A. Mayo-Iscar, "A review of robust clustering methods," *Advances in Data Analysis and Classification*, vol. 4, pp. 89–109, 2010.
- [21] G. E. P. Box and D. R. Cox, "An analysis of transformations," Journal of the Royal Statistical Society Series B: Statistical Methodology, vol. 26, no. 2, pp. 211–243, 1964, publisher: Oxford University Press.
- [22] P. Virtanen, R. Gommers, T. E. Oliphant, M. Haberland, T. Reddy, D. Cournapeau, E. Burovski, P. Peterson, W. Weckesser, J. Bright, S. J. van der Walt, M. Brett, J. Wilson, K. J. Millman, N. Mayorov, A. R. J. Nelson, E. Jones, R. Kern, E. Larson, C. J. Carey, İ. Polat, Y. Feng, E. W. Moore, J. VanderPlas, D. Laxalde, J. Perktold, R. Cimrman, I. Henriksen, E. A. Quintero, C. R. Harris, A. M. Archibald, A. H. Ribeiro, F. Pedregosa, P. van Mulbregt, and SciPy 1.0 Contributors, "SciPy 1.0: Fundamental Algorithms for Scientific Computing in Python," Nature Methods, vol. 17, pp. 261–272, 2020.
- [23] S. Seabold and J. Perktold, "Statsmodels: Econometric and statistical modeling with python," *Proceedings of the 9th Python* in Science Conference, vol. 57, 2010, pp. 92–96.
- [24] C. S. Burlingham, N. Sendhilnathan, O. Komogortsev, T. S. Murdison, and M. J. Proulx, "Motor "laziness" constrains fixation selection in real-world tasks," *Proceedings of the National Academy of Sciences*, vol. 121, no. 12, p. e2302239121, 2024.
- [25] O. Sinha, S. Madarshahian, A. Gomez-Granados, M. L. Paine, I. Kurtzer, and T. Singh, "Smooth pursuit eye movements contribute to anticipatory force control during mechanical stopping of moving objects," *Journal of neurophysiology*, vol. 129, no. 6, pp. 1293–1309, 2023.
- [26] K. N. Thakkar and M. Rolfs, "Disrupted corollary discharge in schizophrenia: evidence from the oculomotor system," *Bio-logical Psychiatry: Cognitive Neuroscience and Neuroimaging*, vol. 4, no. 9, pp. 773–781, 2019.